



OPEN

Short-chain fatty acids ameliorate imiquimod-induced skin thickening and IL-17 levels and alter gut microbiota in mice: a metagenomic association analysis

Yi-Ju Chen^{1,2,9✉}, Hsiu J. Ho³, Ching-Hung Tseng⁴, Yu-Feng Chen³, Sin-Ting Wang³, Jeng-Jer Shieh⁵ & Chun-Ying Wu^{3,6,7,8,9✉}

Short-chain fatty acids (SCFAs) have been proposed to have anti-inflammatory effects and improve immune homeostasis. We aimed to examine the effects of SCFAs on skin phenotype, systemic inflammation, and gut microbiota in mice with psoriasis-like inflammation. Imiquimod (IMQ)-treated C57BL/6 mice served as the study model. We conducted a metagenomic association study of IMQ-mice treated with SCFAs or anti-IL-17 antibody using whole-genome shotgun sequencing. The associations among SCFA supplements, skin thickness, circulating inflammatory profiles, and fecal microbiota profiles were investigated. The microbiome study was performed using pipelines for phylogenetic analysis, functional gene analysis, and pathway analysis. In IMQ-treated mice, there were increases in skin thickness and splenic weight, as well as unique fecal microbial profiles. SCFAs ameliorated IMQ-induced skin thickening, splenic weight gain, and serum IL-17F levels, with results that were comparable with those receiving anti-IL-17 treatment. IMQ-treated mice receiving SCFAs had greater microbial diversity than mice treated with IMQ alone. SCFAs and anti-IL17 treatment were associated with alteration of gut microbiota, with increased prevalences of *Oscillospiraceae* and *Lachnospiraceae* and decreased prevalences of *Muribaculaceae* and *Bacteroides*, which have been predicted to be associated with increased glycan degradation, phenylalanine metabolism, and xylene degradation. SCFAs may mitigate IMQ-induced skin thickening and IL-17F levels and alter fecal microbiota profiles in IMQ-treated mice.

Keywords Short-chain fatty acids, Microbiota, Imiquimod, Inflammation, Mice model

Abbreviations

CAZY	Carbohydrate active enzyme
COG	Clusters of orthologous groups
EC	Enzyme commission
FDR	False discovery rate
FMT	Fecal microbial transplantation
IBD	Inflammatory bowel disease
IBS	Irritable bowel syndrome
KO	KEGG orthology

¹Department of Dermatology, Taichung Veterans General Hospital, Taichung, Taiwan. ²Department of Post-Baccalaureate Medicine, College of Medicine, National Chung Hsing University, Taichung, Taiwan. ³Institute of Bioinformatics and Biomedicine, National Yang Ming Chiao Tung University, Taipei, Taiwan. ⁴Germanck Biotechnology Ltd., No. 21, Keyuan Rd., Situn Dist., Taichung, Taiwan. ⁵Institute of Biomedicine, National Chung Hsing University, Taichung, Taiwan. ⁶Division of Translational Research, Department of Medical Research, Taipei Veterans General Hospital, Taipei, Taiwan. ⁷Faculty of Medicine and Graduate Institute of Clinical Medicine, National Yang Ming Chiao Tung University, Taipei, Taiwan. ⁸Department of Public Health and Graduate Institute of Clinical Medical Sciences, China Medical University, Taichung, Taiwan. ⁹These authors contributed equally: Yi-Ju Chen and Chun-Ying Wu. ✉email: yjchenmd@gmail.com; dr.wu.taiwan@gmail.com

LDA	Linear discriminant analysis
LeSe	Linear discriminant analysis effect size
IMQ	Imiquimod
MAG	Metagenome-assembled genome
ORF	Open reading frame
OTU	Operational taxonomic units
PCoA	Principal coordinate analysis
PsA	Psoriatic arthritis
RA	Rheumatoid arthritis
SCFAs	Short-chain fatty acids
SLE	Systemic lupus erythematosus
TPM	Transcript per million

Psoriasis is a chronic inflammatory disease, with prevalences of 0.2% in Asia, 1.5–1.9% in Europe, and up to 3% in the United States^{1,2}. It is a Th17-related inflammatory skin disease involving skin and joints that is characterized by widespread skin lesions with thick scales and arthritis that may cause significant physical and psychological burdens¹. Psoriasis is associated with multiple comorbidities, including cardiovascular diseases, metabolic syndrome, depression, and inflammatory bowel diseases (IBD)³. It has been suggested that gut microbiota alterations are linked to psoriasis and its systemic comorbidities, severity, and response to biologic treatment^{4–9}.

Psoriasis, psoriatic arthritis, IBD, and obesity have been linked to decreased levels of short-chain fatty acid (SCFA)-producing bacteria, such as *Prevotella*, *Akkermansia*, and *Faecalibacterium*^{10–15}. As the end products of bacterial anaerobic fermentation of dietary fiber, SCFAs, especially propionate and butyrate, bear anti-inflammatory properties, inducing regulatory T cells in the colon and modulating the function of intestinal immune homeostasis¹⁶. Lower fecal or serum SCFA levels, which correspond to significant reductions in the abundance of SCFA-producing bacteria, have been observed in atopic dermatitis^{17,18}, but are not as well characterized in psoriasis¹⁹. Lu et al. recently demonstrated that probiotics mitigate psoriasis-related inflammation. Effective strains of probiotics for alleviating pathologic skin changes and reducing skin inflammation significantly increased SCFA levels in a psoriasis-like mice model study²⁰. The effects of SCFAs on psoriasis-related inflammation are worth further investigation.

In this study, the effects of SCFAs on skin and systemic inflammation and gut microbiome profiles were investigated using imiquimod (IMQ)-treated mice model. We implemented pipelines for phylogenetic analysis, functional gene analysis, and pathway analysis to investigate the associations among these profiles. The results were compared with the effects of anti-IL-17 antibodies on IMQ-treated mice model.

Materials and methods

Study design

The effects of SCFAs alone on experimental and control mice were first investigated in a pilot study ($N=3$ for each group). We then conducted two-stage experiments. In the first stage, we compared the effects of SCFAs on an IMQ-induced psoriasis-like inflammation mouse model. Experimental mice were divided into four groups ($N=16$): those given drinking water with SCFAs plus topical phosphate buffered saline (PBS) ($n=3$), those given SCFAs plus IMQ ($n=5$), those given ordinary drinking water without SCFAs plus topical PBS ($n=3$), and those given ordinary drinking water without SCFAs plus topical IMQ ($n=5$) (Supplementary Fig. S1A). In the second stage, the effects of anti-IL17 treatment on IMQ mice were compared in the presence and absence of SCFAs. Experimental mice were divided into eight groups ($n=40$) depending on SCFA supplementation or anti-IL17 treatment. Non-SCFA supplementation groups included IMQ plus IgG-isotype ($n=5$), IMQ plus anti-IL17 ($n=5$), PBS plus anti-IL17 ($n=5$), and PBS plus IgG-isotype ($n=5$). SCFA groups included SCFAs with IMQ plus IgG-isotype ($n=5$), SCFAs with IMQ plus anti-IL17 ($n=5$), SCFAs with PBS plus anti-IL17 ($n=5$), and SCFAs with PBS plus IgG-isotype ($n=6$) (Supplementary Fig. S1B). To ensure consistent results, each experiment was replicate as needed. Comparisons among groups were performed for skin thickness, organ weights, inflammatory cytokine profiles, and fecal microbiota. Animal management and treatment protocols are described below.

Animal management

All experimental procedures were approved by the Institutional Animal Care and Utilization Committee (IACUC) of Taichung Veterans General Hospital (La-1091737) and performed in accordance with institutional guidelines. Male C57BL/6JNarl mice, aged four weeks, were obtained from the National Laboratory Animal Center (Taipei, Taiwan). They were initially housed in separate cages (3–5 mice per cage, L320*W215*H130mm, SHINETEH) with free access to water and food. The mice in the non-SCFA supplementation groups were provided with standard chow (5001, Laboratory Rodent Diet, USA) and the mice in the SCFA groups were provided with standard chow plus SCFA supplements (Sigma, Germany). Housing conditions included a constant temperature of $22 \pm 1^{\circ}\text{C}$ and a regular 12-h light/dark cycle (lights on 8 PM to 8 AM, with Snai-chip #1511 bedding, Young Li). After three days of acclimatization, the 4-week-3-day-old mice received antibiotics for two days and standard chow (5001, Laboratory Rodent Diet) for 21 days or standard chow with SCFA supplements. The 7-week-5-day-old mice were reallocated to different groups in each arm in separate experiments.

Prior to experiments, the mice were randomly distributed among the groups to ensure a comparable average body weight in each group. Investigators were not blinded during the experiments and analyses.

IMQ treatment and administration

A daily topical dose of 80 mg of commercially available IMQ cream (5%) (Aldara; 3 M Health Care, Leicestershire, UK) was applied to the shaved back and right ear for seven consecutive days, translating into a daily dose of 4 mg of the active compound²¹. Control mice were treated similarly with a control topical PBS solution.

Antibiotics

To avoid background gut microbiota signals, Ciprofloxacin (0.2 g/L) (17,850, Sigma) and Metronidazole (1 g/L) (9,002,409, Cayman)²² were added to drinking water two days before SCFA-supplemented diet or standard chow diet.

SCFA supplement

To explore the effects of SCFAs on inflammation in IMQ-treated mice, experimental mice were provided with standard chow and drinking water supplemented with SCFAs (Sigma Aldrich, Germany) at a final concentration of 150 mM sodium propionate (P1880, Sigma) and 150 mM sodium butyrate (303,410 Sigma) for three weeks before and throughout IMQ treatment^{23,24}. The control mice received standard chow and ordinary drinking water only.

Treatment with IL-17 antibody or isotype of anti-IL-17 antibody

Ultra-LEAF™ Purified anti-mouse anti-IL-17A Antibody (506,945, Biolegend), 100 µg/mouse, was given intraperitoneally every other day during the experimental period, with or without IMQ treatment. To avoid background non-specific signals from target antibodies²⁵, we used IgG-isotype as a negative control. Control mice were injected with isotype (Ultra-LEAF™ Purified Rat IgG1, κ Isotype Ctrl Antibody, 400,431, Biolegend), 100 µg/mouse, every other day in addition to IMQ or PBS application.

Skin thickness, body weight, and tissue weight measurements

To avoid investigator bias, we measured the thicknesses of the right ear and back skin by digital caliper daily during the seven days of IMQ treatment. Skin samples from the ear and back, as well as samples of spleen, liver, and fat, were collected at the end of the experiment and fixed in 10% formaldehyde for H&E staining (Sigma, Germany, Leica Autostainer XL ST5010). Immunohistochemical staining was performed on skin and intestinal epithelia, for tight junction, anti-Claudin 3 antibody (AFFINITY, AF0129) and anti-Claudin 2 Antibody (ab53032, abcam). Each skin section was measured at three random spots and the average skin thickness was calculated. We calculated the thicknesses of the epidermis and dermis of the different treatment groups using Image J software. (National Institute of Health, NIH).

Serum cytokine measurements

Serum samples were collected after the experiments. The cytokine levels of mouse serum (20× diluted) were measured on Multiplex cytokine bead array assay with MILLIPLEX MAP Mouse Cytokine/Chemokine Magnetic Bead Panel (MCYTMMAG-70 KPX32; Millipore). All measurements were performed with a MAGPIX instrument (Luminex, Austin, TX), following the manufacturer's instructions. Data were collected with xPonent software (Luminex). Mann–Whitney U test was used to calculate the significance levels between treatment groups. All results are expressed as mean ± SEM (Standard Error of the Mean). Moreover, p values less than 0.05 were considered significant.

Stool sample collection, DNA extraction, library construction, and metagenomic sequencing

Stool samples were collected and examined before and after IMQ (or PBS) treatment. Stool samples were obtained from each mouse after physical restraint, directly from the rectal aperture to avoid contamination. An Eppendorf tube pre-filled with Inhibitex Buffer, provided in the QIAamp Fast DNA Stool Mini Kit (Qiagen), was used to collect and stabilize the fecal specimen. The collection tube was carefully inserted into the rectal opening, ensuring minimal distress to the tissue. The sample was then secured in the tube, which was subsequently sealed and labeled with the appropriate identification details. Samples were stored at – 20 °C until DNA extraction was performed. The collected fecal sample (about 200 mg) was used for total bacterial DNA extraction with QIAamp Fast DNA Stool Mini Kit (Qiagen, MD, USA) according to the manufacturer's instructions. The quality and quantity of DNA were determined with NanoDrop ND-1000 (Thermo Scientific, Wilmington, DE, USA) and DNA was stored at – 80 °C before library construction and sequencing.

Extracted DNA (about 500 ng) was fragmented to approximately 350 base pairs by Covaris S2 system (Covaris, Inc., Woburn, MA, USA) and then subjected to library construction with Illumina DNA Prep Kit (Illumina, San Diego, CA). Sequencing was performed using Illumina NovaSeq 6000 platform, resulting in paired-end (PE) reads of 150 bp in length.

Metagenomic raw read processing

On a per-sample basis, raw read quality control was performed using the Kneadata pipeline (<https://github.com/biobakery/kneadata>), which integrates Trimmomatic²⁶ for trimming Illumina adaptors and low-quality regions and filtering short reads, as well as Bowtie2²⁷ for identifying and removing host contamination from human hg38 build (or mouse mm10 build) and PhiX genome. Trimmomatic options included “ILLUMINACLIP:NexteraPE-PE.fa:2:30:10” (identifying and removing adapters), “SLIDINGWINDOW:4:20” (trimming low quality region), and “MINLEN:50” (discarding reads shorter than 50 base pairs). After that, reads with low-complexity region

and repeated sequences were identified and removed using Komplexity software (<https://github.com/eclarke/komplexity>) with default settings.

Metagenome assembly, annotation, and binning

Metagenome assembly was performed using MEGAHIT²⁸ to assemble the clean reads into contigs. In terms of taxonomic identification, there were two approaches: (1) read-based taxonomy, which analyzes QC-passed reads using Sourmash²⁹ to estimate relative abundance of taxa based on GTDB taxonomy³⁰ and (2) contig-based taxonomy, which predicts taxonomy of contigs using MMSeqs2^{31,32} easy-taxonomy pipeline and estimates abundance by contigs depth, derived by the jgi_summarize_bam_contig_depths script analyzing bowtie2 alignment that maps the clean reads onto contig.

Open reading frame (ORF) prediction and functional annotation [including the Clusters of Orthologous Groups (COGs) family and Enzyme Commission (EC) number assignment] was performed by subjecting contigs to Prokka³³. ORFs were also analyzed to identify corresponding KEGG Orthology (KO) number, Carbohydrate Active enZyme (CAZy) family, antibiotics gene, and virulence factor using MMSeqs2 easy-search pipeline. MinPath³⁴ was used for pathway reconstruction by analyzing KO (for KEGG pathway) and EC (for MetaCyc pathway)³⁵ profiles of each sample. The abundance of gene families (or categories) was estimated by accumulating ORF depths, which were calculated by tpm_table python script (<https://github.com/EnvGen/toolbox>) based on the number of unique reads mapped on each ORF and presented in units of transcript per million (TPM)³⁶.

Metagenomics binning was performed by MetaBAT³⁷ to cluster contigs into genome “bins” [i.e., metagenome-assembled genomes (MAGs)]. The quality was assessed and taxonomically identified by CheckM lineage-specific workflow³⁸. In addition, the classification of MAGs was based on a voting approach using the contig-based taxonomy of binned contigs, deepening the CheckM-predicted taxonomy in most cases.

Statistical analysis, bioinformatics analysis, and microbial gene function prediction

GraphPad Prism software 10 (GraphPad Software Inc., San Diego, CA, USA) was used to analyze experimental and clinical data. One-way analysis of variance was used for inter-group comparisons. $P < 0.05$ was considered statistically significant. Other statistical analyses were performed using R (<http://www.r-project.org/>), unless otherwise specified. The read- or contig-based taxonomic profiles were imported and handled by R package phyloseq³⁹ and processed for alpha diversity estimation. Beta diversity was analyzed and visualized by principal coordinate analysis (PcoA) via the R package ade4⁴⁰ based on Bray–Curtis distance of species-level relative abundance profile. As for functional profiles, alpha diversity was represented by the number of observed entities. Beta diversity was also analyzed by PcoA based on Bray–Curtis distance of functional genes, families, or relative abundance profiles.

Between-group inertia percentages were tested based on the Monte-Carlo test (with 10,000 permutations) using Bray-Curtis⁴¹, with p values less than 0.05 considered significant. To identify organismal features differentiating communities of fecal microbiota between experimental and control mice, linear discriminant analysis (LDA) effect size (LefSe)⁴² was applied with α of 0.05 (Kruskal–Wallis and Wilcoxon tests) and effect size threshold of 2 on linear discriminant analysis (LDA) using the stand-alone implementation (<https://bitbucket.org/nsegata/lefse>).

The abundances of various gene families of experimental and control mice were scaled by total sum per sample and subjected to enrichment analysis of two-group comparison using several tests, including Wilcoxon signed rank test and ANOVA rank test or Kruskal–Wallis test with a Benjamin-Hochberg false discovery rate (FDR) correction to adjust p values for multiple testing.

The Bioinformatics analyses mentioned above were carried out by Germark Biotechnology Co., Ltd. (Taichung, Taiwan).

The experiments were carried out in accordance with the protocols and approval of the IACUC Taichung Veterans General Hospital, La-1091737.

Approval of animal study and animal welfare

The experiments were carried out in accordance with the protocols approved by the IACUC of Taichung Veterans General Hospital, La-1091737. The present study followed national guidelines of the 3Rs for humane animal treatment and complied with relevant legislation of the Ministry of Agriculture, Taiwan. The study is reported in accordance with ARRIVE guidelines.

Results

SCFAs and anti-IL-17 antibodies ameliorate IMQ-induced skin thickening

We first investigated the effects of SCFA supplements on psoriatic inflammation in IMQ-induced mice model. IMQ-induced inflammation mimics the key characteristics of psoriasis: scaling, erythema, epidermal acanthosis, and infiltration of inflammatory cells in the dermis. Next, we compared the beneficial effects of SCFA supplements to those of anti-IL17 antibodies, a standard treatment for psoriasis, on IMQ-induced inflammation. Mice were administered either SCFA supplements or drinking water for 3 weeks before IMQ exposure. On day 0, mice were subjected to topical IMQ alone or topical IMQ with concurrent administration of anti-IL-17 antibodies for seven days (Supplementary Fig. S1A,B). SCFAs significantly reduced skin thickness gain and skin erythema during the seven days of IMQ application (Fig. 1A,B, Supplementary Fig. S2A–D). H&E staining analysis of treated skin showed consistent results and reduction was most significant in the epidermis (Fig. 1C–E, supplementary Fig. S2E). The beneficial effects of SCFAs on IMQ-induced inflammation were comparable to those of anti-IL-17 treatment.

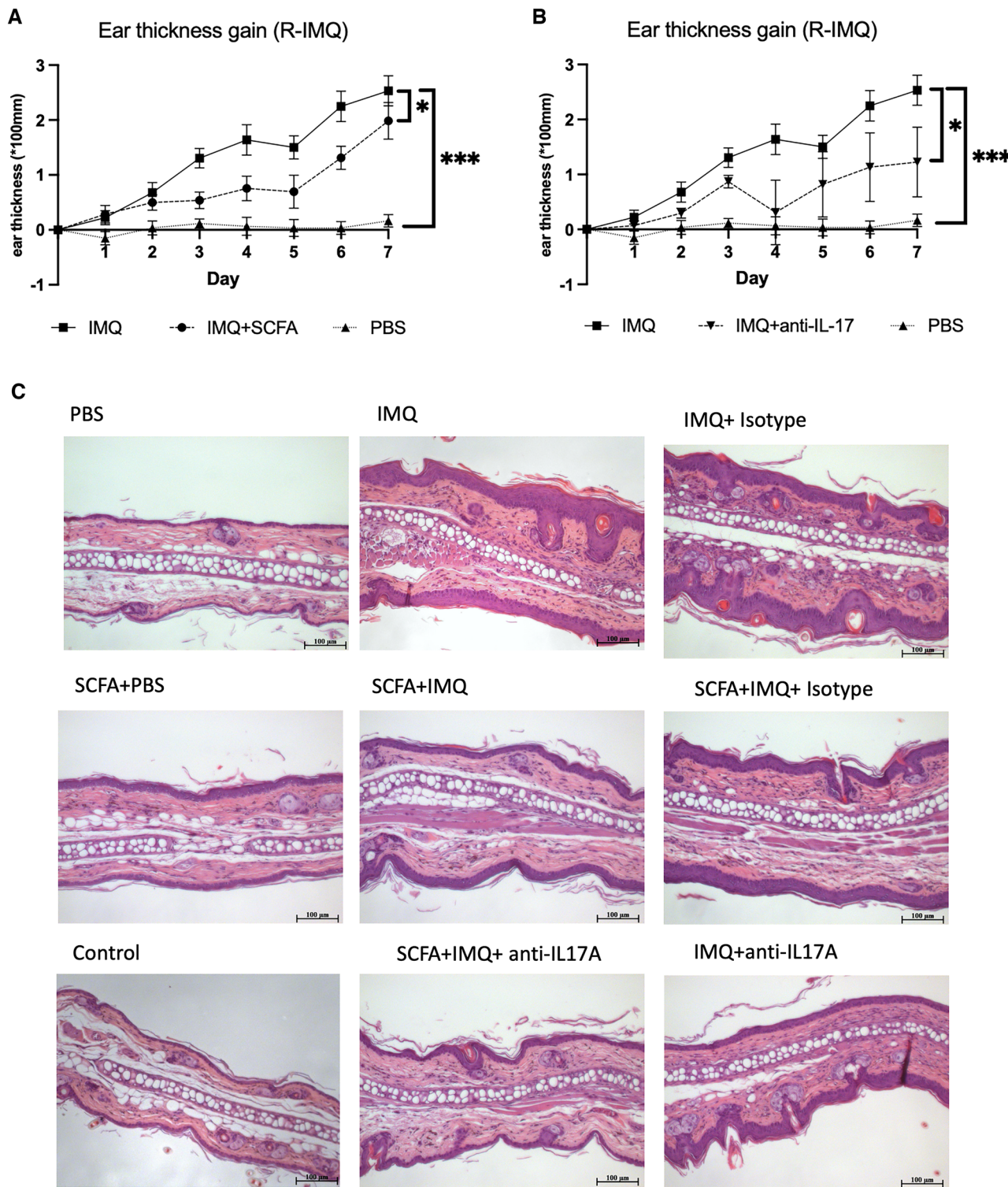
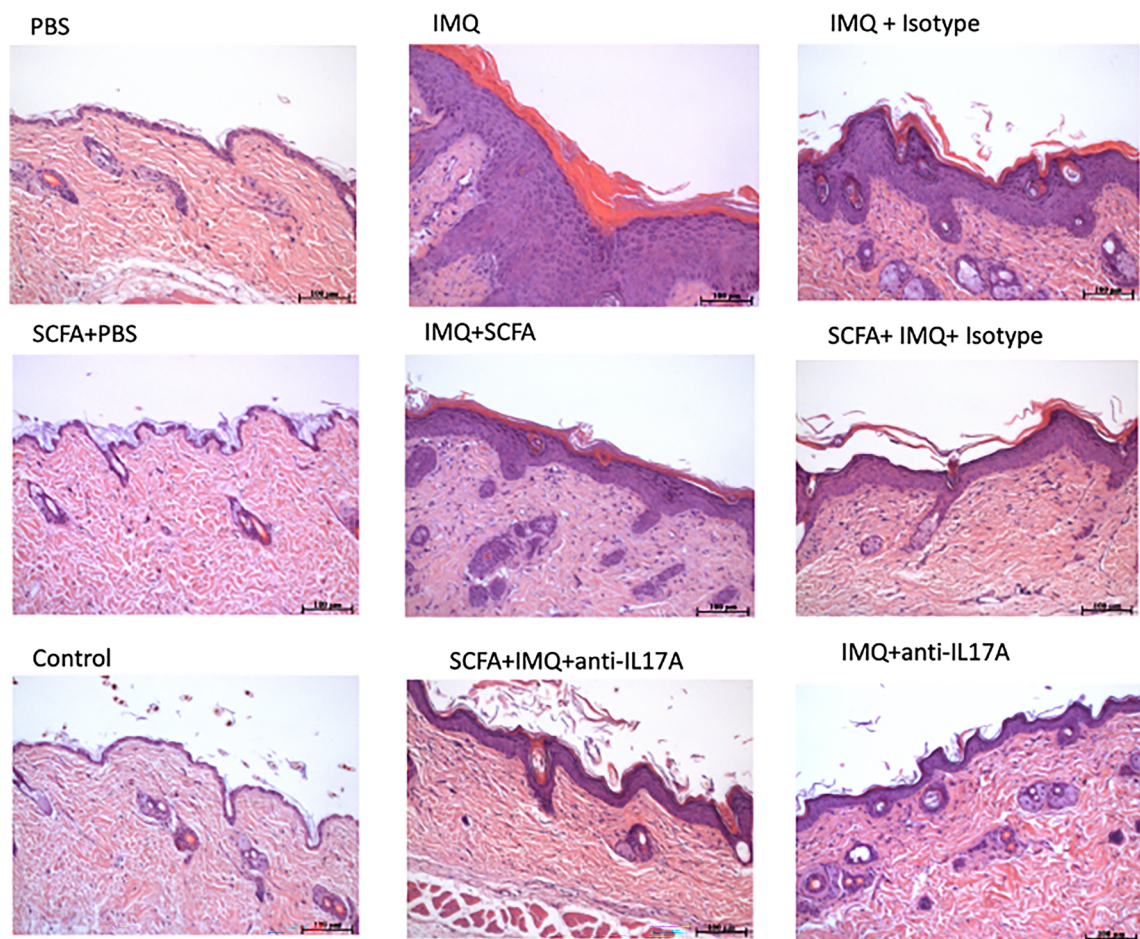
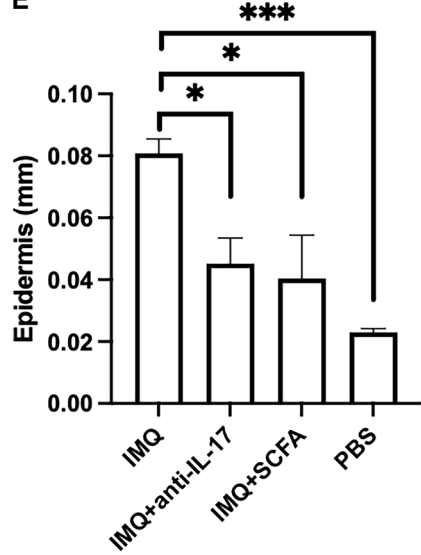
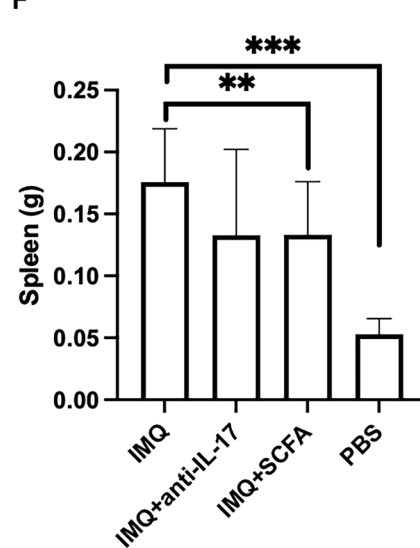


Figure 1. Evaluations of skin thickness and splenic weight alterations following IMQ application in mice, with interventions of SCFAs and anti-IL-17 antibodies. (A) SCFAs and (B) anti-IL-17 antibodies significantly decreased skin thickness gain in IMQ mice. Immunohistochemical analyses of (C) right ear and (D) back skin samples from different treatment groups demonstrated consistent results. (E) The skin thickness changes in epidermis of back were calculated using Image J software. (F) Increase in splenic weight in IMQ-treated mice relative to controls with significant reduction following SCFA and anti-IL17 treatments in IMQ-treated mice. IMQ imiquimod, SCFAs short-chain fatty acids. *The analyses of skin thickness and splenic weight alterations were based on experiments that were performed in triplicate.

D**E****F****Figure 1.** (continued)

SCFAs and anti-IL-17 antibodies ameliorate splenic weight gain and serum IL-17 levels in IMQ-treated mice

Next, we investigated the effects of SCFAs on splenic weight and systemic pro-inflammatory cytokines. IMQ significantly increased splenic weight compared to controls. SCFAs markedly reduced splenic weight gain following IMQ treatment (Fig. 1F, supplementary Fig. S2F–G). There was little change in other organ weights, such as liver and fat, among the treatment groups (Supplementary Fig. S2G–I).

Serum samples were collected at the end of the experiments. IMQ significantly increased serum IL-17F levels compared to controls. Both SCFAs and anti-IL-17 antibodies significantly reduced IL-17F levels induced by IMQ (Fig. 2A). The serum levels of IL-17A were reduced in mice receiving SCFAs or anti-IL-17 antibodies, but without statistical significance (Fig. 2B). There were no changes in TNF- α , IL-22, IL-23, or IL-31 after SCFA or anti-IL-17 treatment (data not presented).

SCFAs and anti-IL-17 antibodies were associated with gut microbial alteration in IMQ-treated mice

Finally, we investigated the functional aspects of the gut microbiome profiles affected by SCFAs. We performed metagenomic sequencing via the following procedures: de novo assembly, prediction of ORFs, clustering and annotation of ORFs, and read mapping to assembled contigs. Based on the results of taxon analysis, we compared the gut microbial profiles among IMQ mice receiving SCFAs, anti-IL-17 antibodies, or isotype control using gene set enrichment analysis.

There were notable differences in fecal microbiota richness, diversity, and distribution between mice treated with SCFAs or anti-IL-17 antibodies and those not treated with SCFAs or anti-IL-17 antibodies following IMQ exposure. In IMQ-isotype mice, SCFAs and anti-IL-17 antibodies were significantly associated with enhanced richness and diversity of fecal microbiota. (Fig. 3A,B), as well as differing fecal microbial compositions (Fig. 3C,D).

The relative abundances of fecal microbiota in different treatment groups are presented in Table 1. Alterations in gut microbiota profiles following SCFA supplementation in IMQ- and IMQ-isotype mice are presented in Fig. 4A,B. The most discriminating OTUs between anti-IL-17 antibody-treated and isotype-treated IMQ mice are presented in Fig. 4C. Increased relative abundances of *Oscillospiraceae* and *Lachnospiraceae* families were found in mice receiving anti-IL-17 antibodies or SCFAs. On the contrary, increased relative abundances of *Mauribaulaceae* and *Bacteroidaceae* were found in mice treated with IMQ plus IgG-isotype alone (Table 1).

Metabolic and signaling pathways of the gut microbiome associated with SCFAs and anti-IL-17 antibodies

The fecal microbial profiles of SCFA-supplemented IMQ-isotype mice were associated with enhanced glycan degradation, phenylalanine metabolism, and xylene degradation (Fig. 4D). On the contrary, the fecal microbial profiles of IMQ-treated mice were associated with enhanced expression of pathways involving carbohydrate metabolism (Fig. 4E). Fecal specimens from IMQ-isotype mice receiving IL-17 antibodies demonstrated enhanced expression of ABC transporter ATP-binding protein (Fig. 4F).

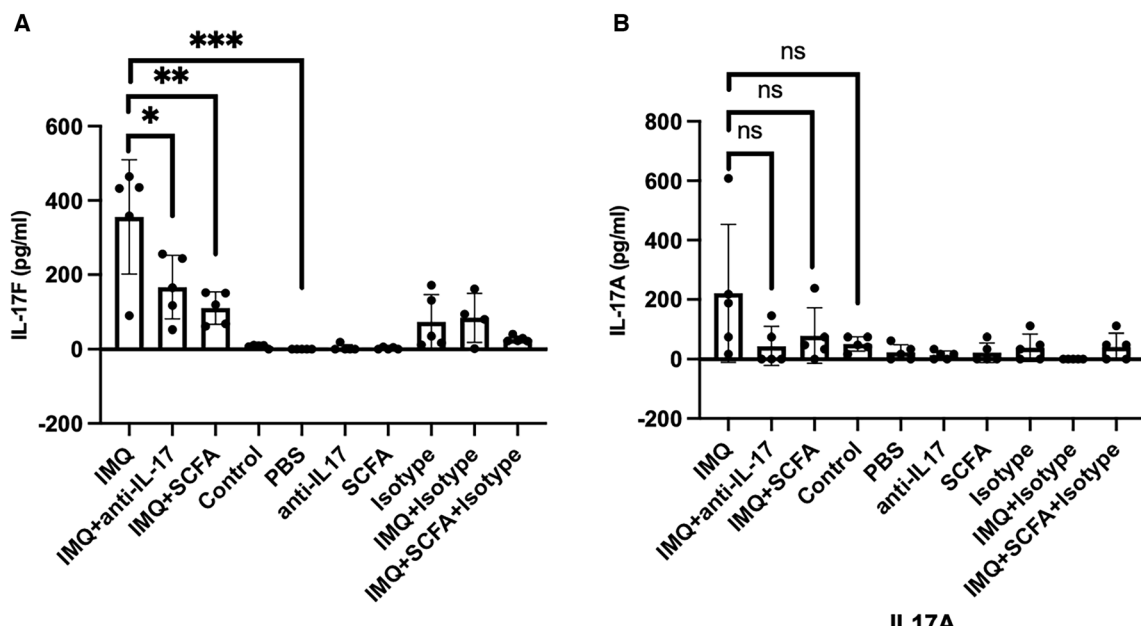


Figure 2. Changes in serum IL-17 after SCFA or anti-IL17 treatment in IMQ mice. SCFAs and anti-IL17 reduced (A) serum IL-17A and (B) IL-17F in IMQ mice. SCFAs, short-chain fatty acids.

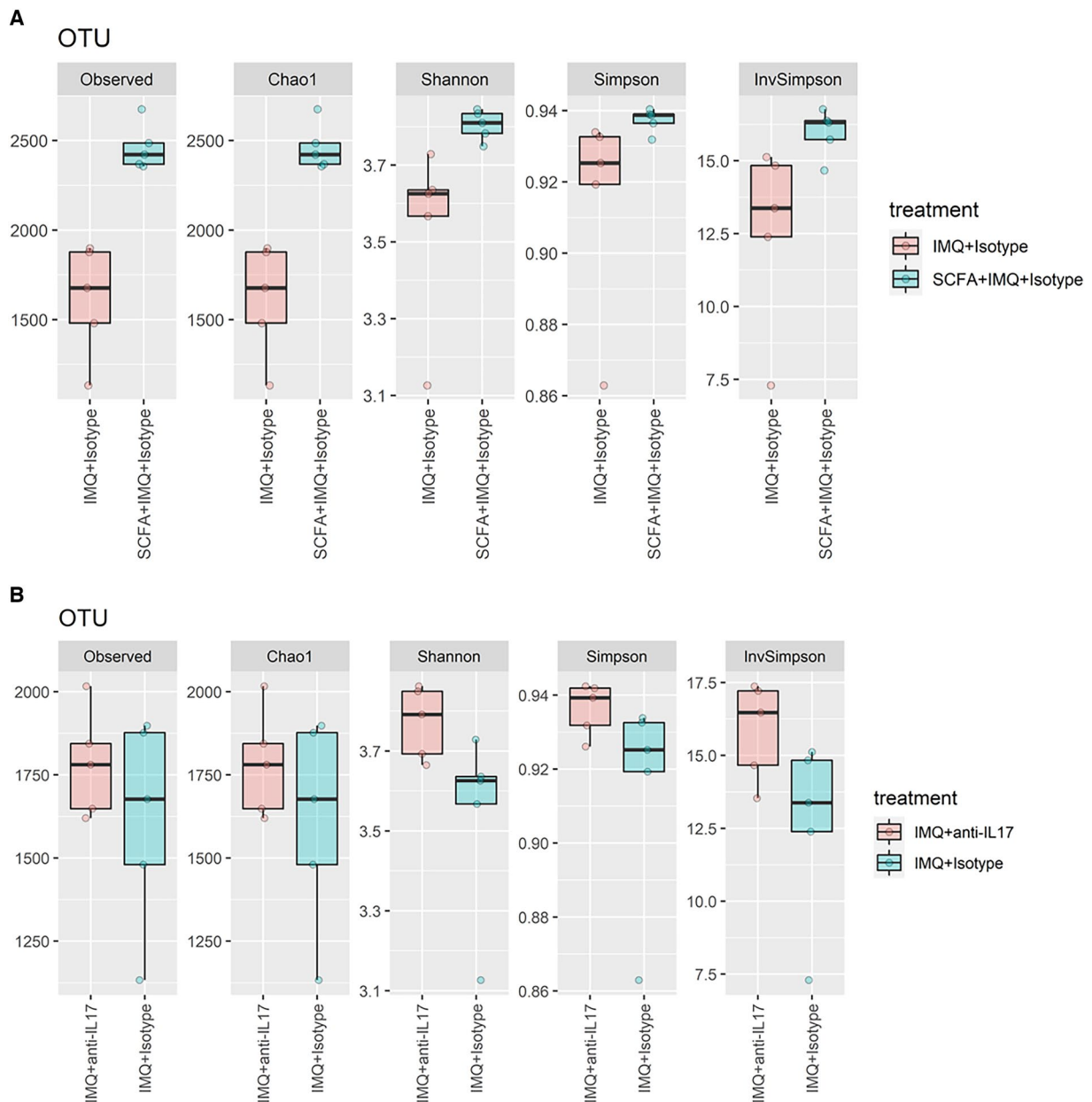
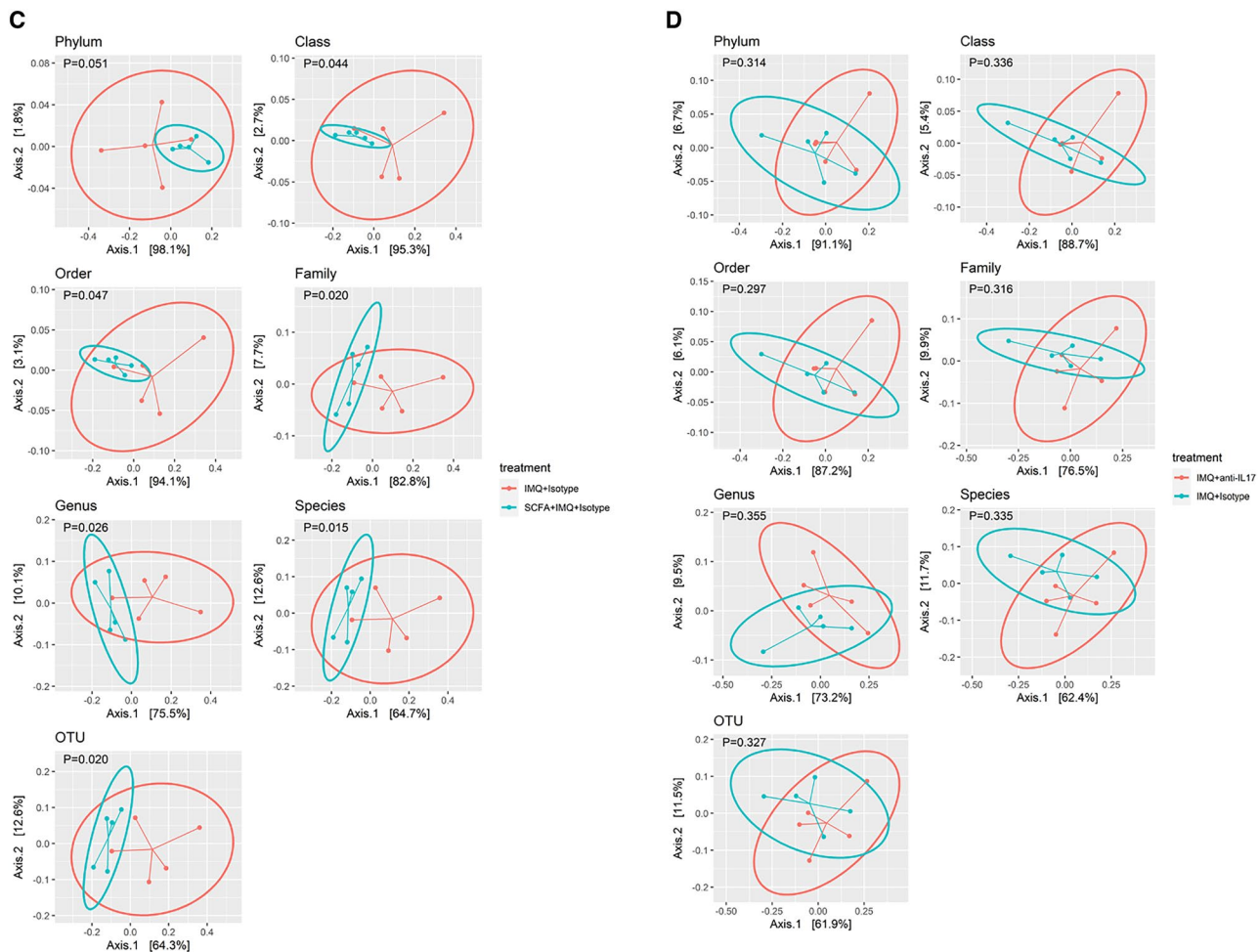


Figure 3. SCFA supplements and IL-17 antagonists enhanced the richness and diversity of fecal microbiota. We compared the α -diversities of fecal microbiota between (A) IMQ mice receiving isotype injections plus SCFA supplements and not receiving SCFA supplements and (B) IMQ mice receiving anti-IL17 or IgG isotype treatment. There were significant differences in the β -diversity of fecal microbiota between IMQ mice receiving (C) IgG isotypes with or without SCFA supplements, but not between (D) IMQ mice with anti-IL17 and IMQ mice with IgG isotype treatment. Between-group inertia percentages were tested using the Monte-Carlo test (with 10,000 permutations) with Bray-Curtis method. p values less than 0.05 were considered significant. The organismal features differentiating communities of fecal microbiota between experimental and control mice were presented by LEfSe, applied with α of 0.05 (Kruskal-Wallis and Wilcoxon tests), as described in the “Methods” section.

Discussion

The results of this study demonstrated that SCFAs are associated with decreased skin thickness and splenic weight gain, as well as reduced expression of IL-17 in IMQ-treated mice. These changes in skin manifestations and inflammatory cytokines resembled the effects of anti-IL-17 antibody treatment. SCFAs were also associated with alterations in gut microbiota, notably increased relative abundances of the *Oscillospiraceae* and *Lachnospiraceae* families. Distinct fecal microbiota have been predicted to be linked to enhanced glycan degradation, phenylalanine metabolism, and xylene degradation based on genetic enrichment analyses.

**Figure 3.** (continued)

SCFAs are primarily produced through anaerobic fermentation by intestinal microbes. The production of SCFAs in the intestinal tract is influenced by factors such as diet, microorganism populations, and the duration of their residence in the intestine⁴³. The anti-inflammatory effect of SCFAs has been reported to be mediated by alleviation of the TNF- α -related TLR4/MyD88/ NF- κ B pathway⁴⁴, which may be involved in the pathogenesis of atherosclerosis⁴⁵. A defect in the function and a reduced number of regulatory T cells have been found in psoriasis. Topical sodium butyrate treatment of psoriatic skin lesions restores the reduced Treg cell number and normalizes the enhanced expression of IL-17A⁴⁶. The results of this study further demonstrated that sodium propionate and sodium butyrate supplements ameliorate IMQ-induced skin and systemic inflammation with decreased IL-17 and TNF- α levels and altered fecal microbiota.

Altered gut microbiota have been proposed to be linked to psoriasis pathogenesis^{5,7}. The impact of SCFAs on fecal microbiota profiles may provide further insight into the underlying mechanism of this association. Previous research has consistently shown that patients with psoriasis and psoriatic arthritis possess unique gut microbial profiles similar to those observed in IBD patients^{6,7}. In our previous studies, we found that psoriasis patients exhibit a distinct fecal microbial signature, which may be linked to carbohydrate transport and chemotaxis, suggesting a connection between metabolic and gastrointestinal comorbidities in psoriasis^{6,7}.

A reduction in butyrate-producing microorganisms has been reported in several diseases, including irritable bowel syndrome (IBS) and psoriasis^{47–49}. Psoriatic patients have been shown to have decreased relative abundances of protective taxa that may produce butyrate in the gut, such as *Parabacteroides* and *Coprococcus*, *Prevotella* and *Ruminococcus*, *Akkermansia muciniphila*, and *Faecalibacterium prausnitzii*^{9–14}, contributing to defects in Treg cells. Furthermore, gut microbial genes encoding the enzymes involved in butyrate synthesis, butyrate kinase, and phosphate butyryl transferase are less abundant in psoriatic patients^{50,51}. These observations support the beneficial role of SCFAs in psoriasis management.

In the present study, we found increased abundances of *Oscillospiraceae* and *Lachnospiraceae* in IMQ-mice receiving anti-IL-17 antibodies and SCFAs. *Oscillospiraceae* butyrate-producing bacteria have anti-inflammatory effects⁵². Several studies have reported that *Oscillospiraceae* is strongly associated with leanness or lower BMI in children and adults. Although controversial, in animal studies *Oscillospiraceae* has been shown to be negatively associated with obesity, type 2 diabetes mellitus (DM), metabolic syndrome, Parkinson's disease, and ulcerative colitis^{52,53}.

Phylum	Class	Order	Family	IMQ	IMQ + aIL17	IMQ + Iso	SCFA + IMQ	SCFA + IMQ + aIL17	SCFA + IMQ + Iso
Firmicutes	Clostridia	Eubacteriales	Oscillospiraceae	14.19341	14.19224	11.58877	17.45899	23.98709	17.1067
Bacteroidetes	Bacteroidia	Bacteroidales	Muribaculaceae	10.82493	11.10455	13.71287	9.99587	4.93656	7.10649
Firmicutes	Clostridia	Eubacteriales	Lachnospiraceae	6.62055	6.16387	3.70137	6.06221	4.18814	7.99925
Firmicutes	Clostridia	Eubacteriales	Clostridiaceae	2.17958	2.19862	1.75696	2.62707	2.22566	2.15887B
Bacteroidetes	Bacteroidia	Bacteroidales	Bacteroidaceae	1.30752	1.52757	1.69125	0.7104	0.45639	1.32308
Bacteroidetes	Bacteroidia	Bacteroidales	Rikenellaceae	1.15702	0.7979	0.58274	0.70203	0.61276	2.22529
Bacteroidetes	Bacteroidia	Bacteroidales	Porphyromonadaceae	0.92118	0.43925	0.46214	0.6631	0.42999	0.64796
Proteobacteria	Deltaproteobacteria	Desulfovibrionales	Desulfovibrionaceae	0.67071	3.47398	2.83279	0.63127	0.67471	0.6576
Bacteroidetes	Bacteroidia	Bacteroidales	Prevotellaceae	0.64314	0.84409	1.45715	0.61149	0.52556	0.7114
Proteobacteria	Epsilonproteobacteria	Campylobacterales	Helio bacteraceae	0.40618	0.82652	0.73416	0.25828	0.15987	0.20081
Actinobacteria	Coriobacteria	Eggerthellales	Eggerthellaceae	0.22574	0.09395	0.05764	0.27046	0.21426	0.04181
Firmicutes	Clostridia	Eubacteriales	Eubacteriaceae	0.18135	0.15001	0.097	0.23011	0.10182	0.37058
Bacteroidetes	Bacteroidia	Bacteroidales	Tannerellaceae	0.15732	0.55902	0.61489	0.17055	0.08736	0.26504
Proteobacteria	Gammaproteobacteria	Enterobacterales	Enterobacteriaceae	0.14528	0.37665	0.09537	0.44915	0.40987	0.28605
Verrucomicrobia	Verrucomicrobiae	Verrucomicrobiales	Akkermansiaceae	0.14145	0.0084	0.25464	0.00514	0.0033	0.00631
Proteobacteria	Betaproteobacteria	Burkholderiales	Sutterellaceae	0.13496	0.31388	0.36529	0.155589	0.08847	0.08597
Firmicutes	Bacilli	Lactobacillales	Lactobacillaceae	0.11846	0.01398	0.01192	0.03391	0.00463	0.17589
Bacteroidetes	Bacteroidia	Bacteroidales	Barnesiellaceae	0.09458	0.101	0.14175	0.13432	0.07715	0.14451
Firmicutes	Erysipelotrichia	Erysipelotrichales	Erysipelotrichaceae	0.04049	0.09367	0.05678	0.04707	0.04484	0.04706
Deferribacteres	Deferribacteres	Deferribacterales	Deferribacteraceae	0.00162	0.22566	0.09862	0.0002	0.00006	0.00052

Table 1. The relative abundances of fecal microbial composition in different treatment groups. *aIL-17* anti-IL17 IgG antibody, *IMQ* imiquimod, *Iso* IgG isotype, *SCFA* short-chain fatty acids.

Lachnospiraceae, which are also butyrate-producing bacteria, have been negatively associated with human genetic variants rs11751024 that have been linked to several clinical traits including psoriasis, type 1 DM, and cardiovascular diseases⁵⁴. One recent mouse study demonstrated that sleep deprivation causes dysregulation of serum inflammatory profiles, in which IL-1 β is positively correlated with the abundance of *Muribaculaceae* and negatively correlated with the abundance of *Lachnospiraceae*⁵⁵. We postulated that the increased abundances of *Lachnospiraceae* and *Ocilliospiraceae* in SCFA-treated mice correlate well with improvements in inflammatory profiles, such as IL-17.

Based on the alterations in fecal microbiota profiles, a number of metabolic pathways of SCFA supplementation and anti-IL17 treatment have been identified on genetic enrichment analyses, including glycan degradation and amino acid metabolism, such as phenylalanine metabolism. Glycan degradation plays a critical role in maintaining intestinal integrity. Deficiencies in enzymes may be involved in gut dysbiosis⁵⁶, resulting in conditions such as IBD and IBS⁵⁶. The beneficial effects of SCFAs in psoriasis might be linked to restored intestinal barrier integrity. Phenylalanine, found in protein-rich foods like milk, eggs, and meat, impairs insulin signaling and inhibits glucose uptake in type 2 diabetes mice model⁵⁷. Phenylalanine is also a precursor for several proteins and neurotransmitters, such as tyrosine, dopamine, norepinephrine, and epinephrine⁵⁸. The dysregulation of these neurotransmitters has been reported to be involved in depression⁵⁹ and schizophrenia⁶⁰. However, these results were based on mice genetic enrichment analyses only. Whether or not there is an association with human psoriasis requires further study.

The alterations in fecal microbiota may not solely be attributed to SCFAs but, rather, multiple factors. Age, sex, host genetic background, infection, use of antibiotics, probiotics or prebiotics, dietary patterns, and environment, such as cage factors, all affect the composition of fecal microbiota. Due to lack of germ-free laboratory conditions, we utilized short-term antibiotics²¹ to prevent background microbiota signals before experiments. We ensured uniformity among the study mice by selecting mice of the same age, sex, and species. Additionally, mice in the same experimental group were housed in a single cage, where they were provided with identical bedding materials throughout the experiment. This standardization minimized variability and controlled for environmental factors. We aimed to avoid all background biases in interpreting our experimental results. We also analyzed the stool samples before and after various treatments. Although there were some differences in fecal microbial diversity and richness before various treatments (Supplementary Fig. S3), they did not affect the trends that emerged at the end of the experiments.

SCFAs are important for maintaining intestinal epithelial homeostasis and integrity⁶¹. However, we did not find significant losses of epithelial tight junction expression, Claudin-3 or Claudin-2 (representing disturbance of epithelial barrier integrity), with IMQ alone in either skin or intestine (Supplementary Fig. S4A–C).

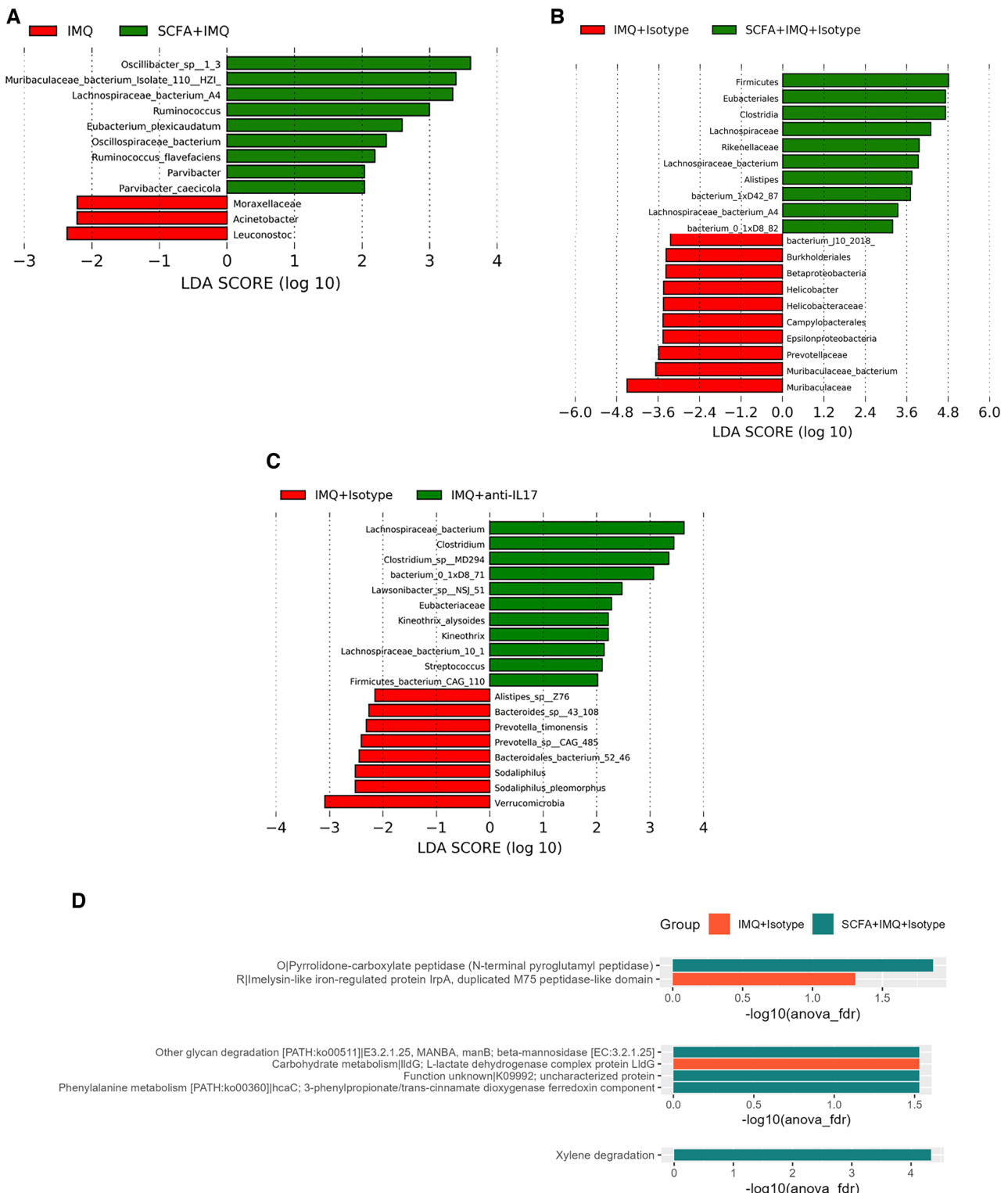


Figure 4. The discriminating microbial species and discriminating metabolic pathways of IMQ mice receiving: (A) SCFAs, (B) anti-IL17, or (C) combination SCFAs and anti-IL17 treatment. The discriminating metabolic pathways in IMQ mice enhanced by (D) SCFA supplements or (E) anti-IL17 treatment and (F) the top 20 discriminating genes after SCFAs. The abundances of various gene families between experiments were scaled by total sum per sample and subjected to enrichment analysis of two-group comparison using several tests, including Wilcoxon signed rank test, ANOVA rank test, or Kruskal-Wallis test with a Benjamin-Hochberg false discovery rate (FDR) correction to adjust p values for multiple testing.

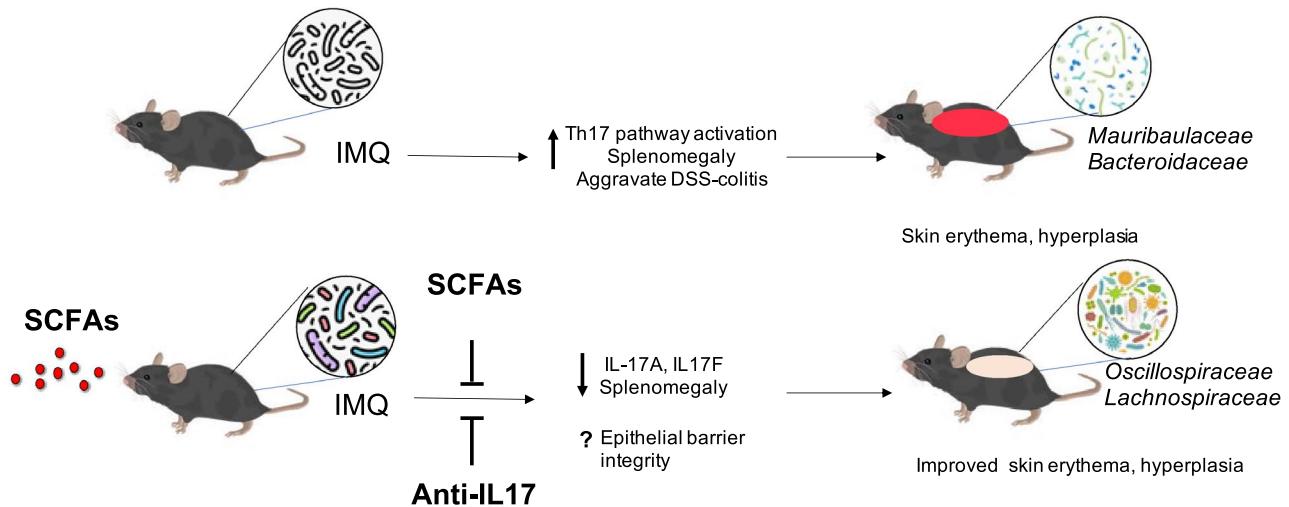


Figure 5. The proposed schematic figure of the mechanisms of SCFA on IMQ-treated mice. IMQ significantly induces skin erythema and hyperplasia via enhanced expression of circulating IL-17 and fecal microbiota alterations. SCFAs may reduce the circulating IL-17F and TNF-alpha, alter the fecal microbiota profiles, and increase the prevalences of *Oscillospiraceae* and *Lachnospiraceae*. IMQ imiquimod, SCFA short-chain fatty acids.

SCFA-associated improvements in IMQ-induced epithelial integrity disturbances may not have been adequately assessed in the current study. However, the results were consistent with prior studies. IMQ alone may not cause intestinal inflammation but can aggravate the severity of dextran sodium sulfate (DSS)-induced colitis^{5,62}. These studies have suggested a two-hit hypothesis for colitis development in IMQ-mice: psoriasis-induced altered gut homeostasis and a secondary environmental challenge. Further experiments using the DSS-colitis model may be helpful. The role of gut microbiota alterations in the beneficial effects of SCFAs on psoriasis-like inflammation remains to be explored. Based on the results of the current study, we propose a schematic mechanism of SCFA effects on psoriasis-like inflammation (Fig. 5).

There are several limitations to the present study. First, our results may only refer to acute skin inflammation in IMQ mice model. This study was conducted using a limited number of mice. The cage factor issue is difficult to exclude. Therefore, the results may not be generalizable to other species or experimental designs and need further validation. Lack of blinding was a concern in collecting clinical data in the present study. To avoid investigator bias, we measured skin thickness in different treatment groups with a digital caliper. Each skin section was measured at three random spots, and the average skin thickness was calculated. In addition, we did not measure the fecal or circulatory metabolite levels in mice. The association of metabolic pathways involving psoriasis-like mice based on gene enrichment analysis may need further investigation.

Nevertheless, the results of this study provide valuable insights into the effects of SCFAs on skin thickness, circulatory IL-17 levels, and fecal microbiota profiles.

In conclusion, SCFAs are associated with anti-inflammatory effects on cutaneous and systemic inflammation in IMQ-treated mice. These effects may be linked to alterations in gut microbiota.

Data availability

Raw sequencing data files of experimental samples have been deposited in NCBI affiliated with BioProject PRJNA1010388.

Received: 15 October 2023; Accepted: 10 July 2024

Published online: 30 July 2024

References

- Griffiths, C. E. M., Armstrong, A. W., Gudjonsson, J. E. & Barker, J. N. W. N. Psoriasis. *Lancet* **397**(10281), 1301–1315 (2021).
- Armstrong, A. W. *et al.* Psoriasis prevalence in adults in the United States. *JAMA Dermatol.* **157**(8), 940–946 (2021).
- Takeshita, J. *et al.* Psoriasis and comorbid diseases: Epidemiology. *J. Am. Acad. Dermatol.* **76**, 377–390 (2017).
- Zakostelska, Z. *et al.* Intestinal microbiota promotes psoriasis-like skin inflammation by enhancing Th17 response. *PLoS one*. **11**, e0159539 (2016).
- Kiyohara, H. *et al.* Toll-like receptor 7 agonist-induced dermatitis causes severe dextran sulfate sodium colitis by altering the gut microbiome and immune cells. *Cell Mol. Gastroenterol. Hepatol.* **7**(1), 135–156 (2018).
- Ricchetta, A. G., Grassi, S., Moliterni, E., *et al.* Increased intestinal barrier permeability in patients with moderate to severe plaque-type psoriasis. *J. Dermatol.* **47**(10), e366–e.368 (2020).
- Scher, J. U. *et al.* Decreased bacterial diversity characterizes the altered gut microbiota in patients with psoriatic arthritis, resembling dysbiosis in inflammatory bowel disease. *Arthritis Rheumatol.* **67**, 128–139 (2015).
- Chen, Y. J. *et al.* Intestinal microbiota profiling and predicted metabolic dysregulation in psoriasis patients. *Exp. Dermatol.* **27**(12), 1336–1343 (2018).
- Yeh, N. L., Hsu, C. Y., Tsai, T. F. & Chiu, H. Y. Gut microbiome in psoriasis is perturbed differently during secukinumab and ustekinumab therapy and associated with response to treatment. *Clin. Drug Invest.* **39**(12), 1195–1203 (2019).

10. Mima, K. *et al.* Fusobacterium nucleatum and T cells in colorectal carcinoma. *JAMA Oncol.* **1**, 653–661 (2015).
11. Alekseyenko, A. V. *et al.* Community differentiation of the cutaneous microbiota in psoriasis. *Microbiome*. **1**, 31 (2013).
12. Costello, M. E. *et al.* Intestinal dysbiosis in ankylosing spondylitis. *Arthritis Rheumatol.* **67**, 686–691 (2015).
13. Breban, M. *et al.* Faecal microbiota study reveals specific dysbiosis in spondyloarthritis. *Arthritis Rheum. Dis.* **76**, 1614–1622 (2017).
14. Yin, J., Liao, S. X., He, Y., *et al.* Dysbiosis of gut microbiota with reimethylamine-N-oxide level in patients with larger artery atherosclerotic stroke or transient ischemic attack. *J. Am. Heart Assoc.* **4**, e002699 (2015).
15. Derrien, M., Belzer, C. & de Vos, W. M. Akkermansia muciniphila and its role in regulating host functions. *Microb. Pathog.* **106**, 171–181 (2017).
16. Russo, E. *et al.* Immunomodulating activity and therapeutic effects of short chain fatty acids and tryptophan post-biotics in inflammatory bowel disease. *Front. Immunol.* **10**, 2754 (2019).
17. Reddel, S. *et al.* Gut microbiome profile in children affected by atopic dermatitis and evaluation of intestinal persistence of probiotics mixture. *Sci. Rep.* **9**(1), 4996 (2019).
18. Xiao, X. *et al.* The role of short-chain fatty acids in inflammatory skin diseases. *Front. Microbiol.* **13**, 1083432 (2023).
19. Lu, W. *et al.* Potential role of probiotics in ameliorating psoriasis by modulating gut microbiota in imiquimod-induced psoriasis-like mice. *Nutrients* **13**(6), 2010 (2021).
20. Khyshktuev, B. S., Karavaeva, T. M., Fal'ko, E. V. Variability of quantitative changes in short-chain fatty acids in serum and epidermis in psoriasis. *Klin. Lab. Diagn.* **8**, 22.
21. van der Fots, L., Mourits, S., Voerman, J.S.A. *et al.* Advanced characterization of imiquimod-induced psoriasis-like mouse model. *Pharmaceutics*. **2020**;12(9), 789.
22. Luo, D. Q., Wu, H. H., Zhao, Y. K., Liu, J. H. & Wang, F. Different imiquimod creams resulting in differential effects for imiquimod-induced psoriatic mouse models. *Exp. Biol. Med. (Maywood)* **241**(16), 1733–1738 (2016).
23. Lai, Z. L. *et al.* Fecal microbiota transplantation confers beneficial metabolic effects of diet and exercise on diet-induced obese mice. *Sci. Rep.* **8**(1), 15625 (2018).
24. Lucas, S. *et al.* Short-chain fatty acids regulate systemic bone mass and protect from pathological bone loss. *Nat. Commun.* **9**(1), 55 (2018).
25. Mizuno, M., Noto, D., Kaga, N., Chiba, A. & Miyake, S. The dual role of short fatty acid chains in the pathogenesis of autoimmune disease models. *PLoS One* **12**(2), e0173032 (2017).
26. Pollinger, B. *et al.* Th17 cells, not IL-17+ γδ T cells, drive arthritic bone destruction in mice and humans. *J. Immunol.* **186**, 2602–2612 (2011).
27. Gill, P. A., van Zelm, M. C., Muir, J. G. & Gibson, P. R. Review article: short chain fatty acids as potential therapeutic agents in human gastrointestinal and inflammatory disorders. *Aliment Pharmacol. Ther.* **48**(1), 15–34 (2018).
28. Li, D., Liu, C. M., Luo, R., Sadakane, K. & Lam, T. W. MEGAHit: An ultra-fast single-node solution for large and complex metagenomics assembly via succinct de Bruijn graph. *Bioinformatics*. **31**, 1674–1676 (2015).
29. Pierce, N. T., Irber, L., Reiter, T., Brooks, P., & Brown, C. T. Large-scale sequence comparisons with sourmash. *F1000Res.* **8**, 1006 (2019).
30. Parks, D. H. *et al.* A standardized bacterial taxonomy based on genome phylogeny substantially revises the tree of life. *Nat. Biotechnol.* **36**, 996–1004 (2018).
31. Steinegger, M. & Soding, J. MMseqs2 enables sensitive protein sequence searching for the analysis of massive data sets. *Nat. Biotechnol.* **35**, 1026–1028 (2017).
32. Mirdita, M., Steinegger, M., Breitwieser, F., Soding, J. & Levy, K. E. Fast and sensitive taxonomic assignment to metagenomic contigs. *Bioinformatics*. **37**, 3029–3031 (2021).
33. Seemann, T. Prokka: Rapid prokaryotic genome annotation. *Bioinformatics*. **30**, 2068–2069 (2014).
34. Ye, Y. & Doak, T. G. A parsimony approach to biological pathway reconstruction/inference for genomes and metagenomes. *PLoS Comput. Biol.* **5**, e1000465 (2009).
35. Caspi, R. *et al.* The MetaCyc database of metabolic pathways and enzymes—a 2019 update. *Nucleic Acids Res.* **48**, D445–D453 (2020).
36. Wagner, G. P., Kin, K. & Lynch, V. J. Measurement of mRNA abundance using RNA-seq data: RPKM measure is inconsistent among samples. *Theory Biosci.* **131**, 281–285 (2012).
37. Kang, D. D. *et al.* MetaBAT 2: An adaptive binning algorithm for robust and efficient genome reconstruction from metagenome assemblies. *PeerJ* **7**, e7359 (2019).
38. Parks, D. H., Imelfort, M., Skennerton, C. T., Hugenholtz, P. & Tyson, G. W. CheckM: assessing the quality of microbial genomes recovered from isolates, single cells, and metagenomes. *Genome Res.* **25**, 1043–1055 (2015).
39. McMurdie, P. J. & Holmes, S. phyloseq: An R package for reproducible interactive analysis and graphics of microbiome census data. *PLoS One*. **8**, e61217 (2013).
40. Dray, S. & Dufour, A.-B. The ade4 package: Implementing the duality diagram for ecologists. *J. Stat. Softw.* **22**, 1–20 (2007).
41. Bray, J. R. & Curtis, J. T. An ordination of the upland forest communities of Southern Wisconsin. *Ecol. Monogr.* **27**, 326–347 (1957).
42. Segata, N. *et al.* Metagenomic biomarker discovery and explanation. *Genome Biol.* **12**, R60 (2011).
43. Lu, H. *et al.* Butyrate-producing *Eubacterium rectale* suppresses lymphomagenesis by alleviating the TNF-induced TLR4/MyD88/NF-κB axis. *Cell Host Microbes*. **30**(8), 1139–1150 (2022).
44. Lundberg, A. M. *et al.* Toll-like receptor 3 and 4 signalling through the TRIF and TRAM adaptors in haematopoietic cells promotes atherosclerosis. *Cardiovasc. Res.* **99**(2), 364–373 (2013).
45. Schwarz, A., Philippsen, R. & Schwarz, T. Induction of regulatory T cells and correction of cytokine imbalance by short-chain fatty acids: Implications for psoriasis therapy. *J. Invest. Dermatol.* **141**(1), 95–104.e2 (2021).
46. Hidalgo-Cantabrana, C. *et al.* Gut microbiota dysbiosis in a cohort of patients with psoriasis. *Br. J. Dermatol.* **181**(6), 1287–1295 (2019).
47. Pozuelo, M. *et al.* Reduction of butyrate- and methane-producing microorganisms in patients with Irritable Bowel Syndrome. *Sci. Rep.* **5**, 12693 (2015).
48. Čipčík Paljetak, H. *et al.* Gut microbiota in mucosa and feces of newly diagnosed, treatment-naïve adult inflammatory bowel disease and irritable bowel syndrome patients. *Gut Microbes*. **14**(1), 2083419 (2022).
49. Trompette, A. *et al.* Gut-derived short-chain fatty acids modulate skin barrier integrity by promoting keratinocyte metabolism and differentiation. *Mucosal. Immunol.* **15**(5), 908–926 (2022).
50. Coppola, S. *et al.* Potential clinical applications of the post-biotic butyrate in human skin diseases. *Molecules*. **27**(6), 1849 (2022).
51. Yang, J. *et al.* Oscillospira—a candidate for the next-generation probiotics. *Gut Microbes*. **13**(1), 1987783 (2021).
52. Wang, J. *et al.* Gut microbiota and transcriptome profiling revealed the protective effect of aqueous extract of *Tetrastigma hemleyanum* leaves on ulcerative colitis in mice. *Curr. Res. Food Sci.* **6**, 100426 (2023).
53. Markowitz, R. H. G. *et al.* Microbiome-associated human genetic variants impact genome-wide disease risk. *Proc. Natl. Acad. Sci. U S A.* **119**(26), e2200551119 (2022).
54. Zhang, M., Zhang, M., Kou, G. & Li, Y. The relationship between gut microbiota and inflammatory response, learning and memory in mice by sleep deprivation. *Front. Cell Infect. Microbiol.* **13**, 1159771 (2023).
55. Kudelka, M. R., Stowell, S. R., Cummings, R. D. & Neish, A. S. Intestinal epithelial glycosylation in homeostasis and gut microbiota interactions in IBD. *Nat. Rev. Gastroenterol. Hepatol.* **17**(10), 597–617 (2020).

56. Zhou, Q. *et al.* Phenylalanine impairs insulin signaling and inhibits glucose uptake through modification of IR β . *Nat. Commun.* **13**(1), 4291 (2022).
57. Fernstrom, J. D. & Fernstrom, M. H. Tyrosine, phenylalanine, and catecholamine synthesis and function in the brain. *J. Nutr.* **137**(6 Suppl 1), 1539S–1547S (2007).
58. Nutt, D. J. Relationship of neurotransmitters to the symptoms of major depressive disorder. *J. Clin. Psychiatry.* **69**(Suppl E1), 4–7 (2008).
59. Hirvonen, J. & Hietala, J. Dysfunctional brain networks and genetic risk for schizophrenia: Specific neurotransmitter systems. *CNS Neurosci. Ther.* **17**(2), 89–96 (2011).
60. Chang, C. S. & Kao, C. Y. Current understanding of the gut microbiota shaping mechanisms. *J. Biomed. Sci.* **26**(1), 59 (2019).
61. Liu, P. *et al.* The role of short-chain fatty acids in intestinal barrier function, inflammation, oxidative stress and colonic carcinogenesis. *Pharmacol. Res.* **165**, 105420 (2021).
62. Pinget, G. V. *et al.* Dysbiosis in imiquimod-induced psoriasis alters gut immunity and exacerbates colitis development. *Cell Rep.* **40**(7), 111191 (2022).

Acknowledgements

We would like to thank Germark Biotechnology, Co., Ltd. Taiwan for providing microbiota analyses. This study was supported by the National Science Technology Council, Taiwan (NSTC 108-2314-B-075A-008 and 110-2314-B-075A-008) and Taichung Veterans General Hospital (TCVGH- 1106801C, 1116801C, and 1116802C).

Author contributions

YC, CW, and HJH had full access to all of the data in the study and took responsibility for the integrity of the data and the accuracy of the data analysis. YC and CW conceived of and designed the study. YC, CT, and CW completed the first draft of the manuscript. YFC, ST, and JS supervised and conducted the animal experiments. YFC, ST, HJH, and CT performed the statistical analysis. All authors participated in the acquisition, analysis, and interpretation of data. All authors have read and approved the manuscript.

Funding

This work was supported by grants NSTC 108-2314-B-075A-008 and 110-2314-B-075A-008 and TCVGH- 1106801C, 1116801C, and 1116802C.

Competing interests

The authors declare no competing interests.

Additional information

Supplementary Information The online version contains supplementary material available at <https://doi.org/10.1038/s41598-024-67325-x>.

Correspondence and requests for materials should be addressed to Y.-J.C. or C.-Y.W.

Reprints and permissions information is available at www.nature.com/reprints.

Publisher's note Springer Nature remains neutral with regard to jurisdictional claims in published maps and institutional affiliations.



Open Access This article is licensed under a Creative Commons Attribution-NonCommercial-NoDerivatives 4.0 International License, which permits any non-commercial use, sharing, distribution and reproduction in any medium or format, as long as you give appropriate credit to the original author(s) and the source, provide a link to the Creative Commons licence, and indicate if you modified the licensed material. You do not have permission under this licence to share adapted material derived from this article or parts of it. The images or other third party material in this article are included in the article's Creative Commons licence, unless indicated otherwise in a credit line to the material. If material is not included in the article's Creative Commons licence and your intended use is not permitted by statutory regulation or exceeds the permitted use, you will need to obtain permission directly from the copyright holder. To view a copy of this licence, visit <http://creativecommons.org/licenses/by-nc-nd/4.0/>.

© The Author(s) 2024